

Gravitational Waves

Bashar Karaja

December 22, 2023

Abstract

This project first investigates gravitational wave (GW) data from two significant events, GW190814 and GW170817, recorded by the LIGO detectors at Livingston and Hanford. Fourier analysis revealed multiple noise peaks affecting the signal, and dominating noise at low-frequency. Very short-lived rapid decaying structures are observed in the data due to the increasingly high frequency of the generated gravitational waves as the two body components draw nearer to each other before merging. Signal contributions were concentrated between 50 Hz to 250 Hz across all mergers. Spectrograms pre-filtering or the usage of the Q-transform method showed a chirping peak clearly in GW190814-L1 but almost no visibility to that of GW190814-H1 with both having noise affecting the clarity. Post-filtering and applying Q-transform improved the chirping peak visibility in GW190814-L1, while GW190814-H1 exhibited challenges as before filtering. For GW170817-L1, Q-transform yielded a noisy behavior with no discernible chirping peaks, while GW170817-H1 lost the almost invisible chirping peak entirely. This suggests that Q-transform techniques are effective for massive objects like black holes but less so for lighter objects like neutron stars. The latter has also shown longer merging duration and less sharp peaks than a black hole merger. Matched filtering, however, proved efficient in extracting buried signals from both quiet and noisy GW events, even when signals were faint.

1 Introduction

Gravitational waves, a revolutionary prediction of Albert Einstein's theory of general relativity, have opened a new frontier in astrophysics, enabling the direct observation of cosmic phenomena. One of the most prolific sources of gravitational waves arises from binary systems, where two massive objects orbit each other in a celestial dance. These celestial bodies could be two black holes, two neutron stars, or one black hole and one neutron star orbiting each other. (1)

In principle, both black holes and neutron stars are the remaining of death stars. When a star comes to an end to its life, it results in a supernova explosion, releasing an immense amount of energy, that sometimes briefly outshines an entire galaxy. what happens next is up to the core mass left, if it is then than 4 times that of our sun, the dead star now becomes a neutron star, while if the remaining core is 5 times larger than the mass of our sun, it collapses into a black hole. (2)

This project aims to study the gravitational waves emitted by these celestial bodies, i.e: those formed as binary systems and are in-spiraling each other to finally collide and merge(Coalescence)

2 GW190814 Black Hole Binary System Merger

2.1 Characteristics

On August 14, 2019, at 21:10:39 UTC the LIGO detector detected gravitational waves coming from a compact binary coalescence involving a 22.2-22.4 Solar mass black hole and a 2.50-2.67 solar mass celestial body producing one of the most interesting gravitational waves observed. This binary system now called GW190814 was the first of its type discovered, due to the huge difference between the masses of the two bodies, with a mass ratio of 0.112. As a result, Scientists were confused about what type of the second(smaller) body is. If it is a black hole, then it is the lightest black hole ever detected in a binary system, and if it is a neutron star, then it is the heaviest ever detected. (4)

in the Coming subsections, we will be studying this interesting merger event, i.e: data recorded by both LIGO detectors: Livingston and Hanford, and try to learn more about its wave characteristics.

2.2 Time domain Visualization

Below we will view the raw LIGO data. The graphs in Fig.1 show the raw data representation of both GW190814-L1 recorded by LIGO-Livingston and GW190814-H1 recorded by LIGO-Hanford:

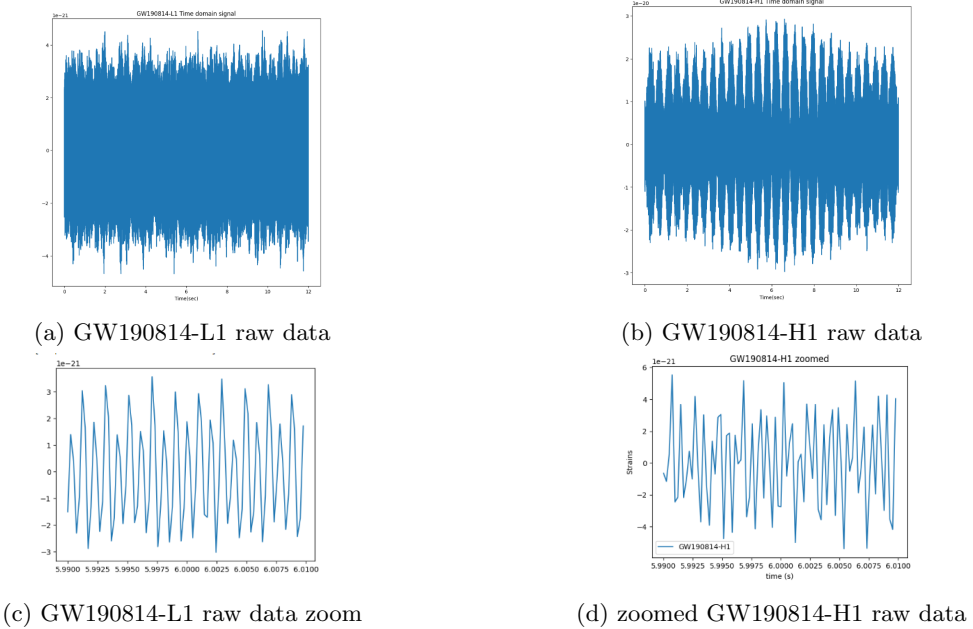


Figure 1: shows the time domain signal of GW190814 raw data

2.2.1 Observation and a Closer view

Notice that the data is very pact if we look at this scale, so we had to zoom into intervals of fractions of seconds to see the gravitational waves clearly as they are rapidly decaying. When zoomed in to one second around GW150914, all you can see is the low-frequency behavior of the noise, since it is much louder than the higher-frequency noise (and signal).

2.2.2 Interpretation of fast decays

The observed gravitational waves exhibit an astonishingly subtle nature, characterized by their remarkably weak amplitudes on the order of 10^{-21} . This feebleness can be attributed to the vast distance of the binary black hole system from Earth, approximately 241 Megaparsecs (Mpc) (4), where 1 Mpc corresponds to 3.09×10^{19} kilometers. The significant spatial separation poses a challenge for LIGO detectors to capture these faint signals effectively.

An intriguing feature in the data structure is the presence of numerous very sharp peaks, indicative of the fast decay of gravitational waves. This phenomenon is common to black hole gravitational wave data, particularly as these waves emanate from the dynamic interplay of colossal celestial bodies, such as black holes and neutron stars, orbiting each other at enormously high speeds. The resulting gravitational waves manifest in the time domain as decaying sharp peaks that dissipate rapidly.

This swift decay is a consequence of the accelerating rotation of the binary black hole system as the two massive objects draw nearer. The intensification of their orbital velocity gives rise to gravitational waves of increasing high frequencies. Consequently, the structures observed in the data exhibit even

briefer lifespans in the time domain as time and frequency are inversely correlated, showing the dynamic and transient nature of celestial events involving massive astronomical bodies.

2.3 Fourier Transform

In this stage, we embark on the computation of the Discrete Fourier transform(5) for the two signals. This analytical process is instrumental in gaining a deeper insight into the signal characteristics, allowing us to unravel the intricate details and discern the underlying structure of the noise. By performing the Fourier transform, we aim to elucidate the signal's frequency components, providing a comprehensive understanding of its composition and facilitating a nuanced examination of the prevailing noise patterns. As given, we take the sampling frequency f_s as: $f_s = 4096\text{Hz}$

Figure.2 shows the modulus spectrum of GW190814-L1 and GW190814-H1 discrete Fourier transform respectively:

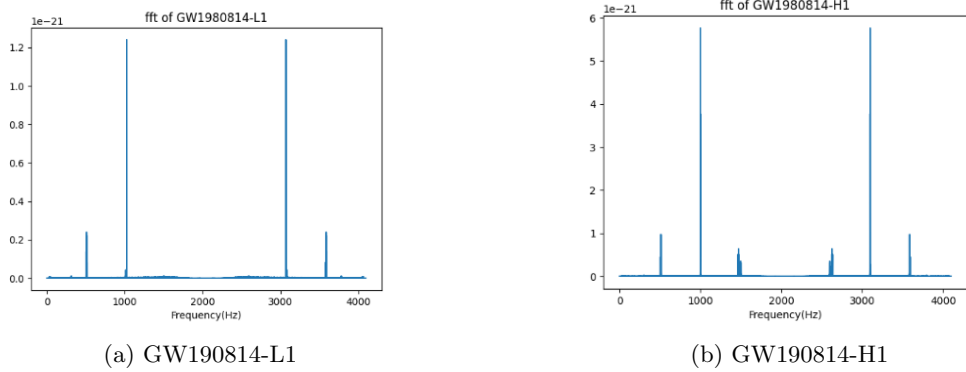


Figure 2: shows the Fourier Transform of GW190814 data

2.3.1 Interpretation

Both data GW190814-L1 and GW190814-H1 show a low-frequency noise all over the signal, in addition to 2 dominating peaks appearing at frequencies: 1000Hz and 3000Hz, and two other smaller peaks at 500Hz and 3500Hz approximately. However, GW190814-H1 shows an extra peaks at the frequencies 1500 Hz and 2500 Hz. All the mentioned peaks are not part of the gravitational waves emitted by the merger but are a result of noise produced by LIGO detectors while recording the data i.e: scattered light at the LIGO Livingston and Hanford detector, in addition to some other factors. Nonetheless, their presence will cause a significant disturbance in the results as they are stronger than the original signal itself. (6)

Furthermore, we found that the most contribution to the data happens at the frequency range between 50 and 250 Hz, and this is very important to notice as it will be of great benefit to us in the coming steps.

2.4 Windowing and Spectrograms

While the Discrete Fourier Transform operates on an entire signal, the Sliding Window Discrete Fourier Transform(SWDFT) (3) takes an ordered sequence of smaller DFTs on contiguous subsets of a signal. The SWDFT is a fundamental tool in time-frequency analysis and is used in a variety of applications, such as spectrogram estimation.

For our data, we used a sliding window of number of points $N_w = 2^{11}$ and a slide number of $N_w/16$ as well as a hanning window to improve our results and then constructed the Spectrogram of the data. (See Figure.3)

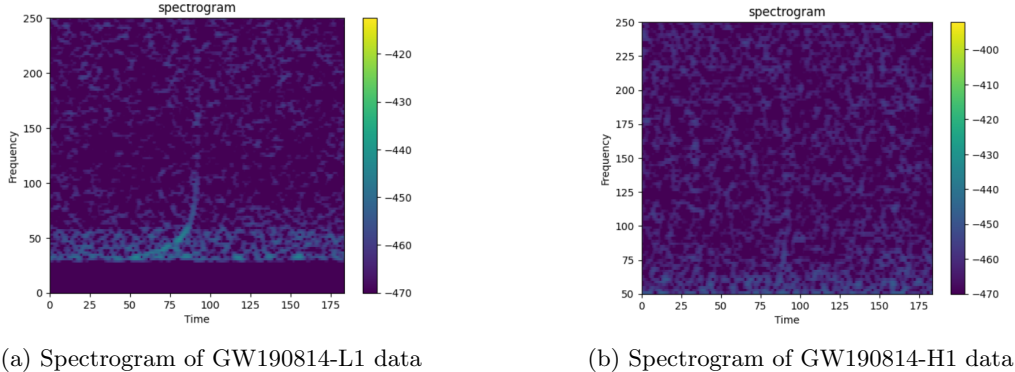


Figure 3: shows the Spectrograms of GW190814 data

2.4.1 Interpretations

from our analysis, we were able to spot the general expected form of the gravitational wave in GW190814-L1, especially the chirping peak at the end, meaning that we have successfully received the general shape of the data. However, there is still the presence of noise which is also captured and visualized. Comparing it to the results of the research paper provided the chirping peak is not as visible as in the paper. Therefore, Implementing filters might help in improving our results and we will be testing this as we proceed in the paper.

A very similar interpretation for GW190814-H1 when it comes to the presence of noise and its effect on the spectrogram, however, there has been almost no detection of the chirping peak(very dim) even though both data are supposed to describe the same merger event, which maybe leads us to conclude that Hanford detector might not be as sensitive in measurements as that of Livingston, or there might have been extra noise where the Hanford detector is.

What's next?

Further analysis is needed i.e: we should apply some filtering on the data to get rid of the noise and finally be able to get a clearer visualization of the signals similar to that in the research paper.

2.5 Filtering the Data from Noise

In this section, we will be performing filtering on the noisy signals we have and then plotting the spectrogram after the data is cleaned. For this, we will be following the steps below:(6)

- 1)High Pass Filtering
- 2)Calculating the Power Spectral Density(PSD)
- 3)Whitening the data
- 4)Band pass Filtering
- 5)Spectrogram

2.5.1 High Pass Filtering

In this section, we applied a high pass filter of threshold frequency = 15Hz. The reason behind this is to suppress the low-frequency noise of the instrument. However, there are still some dominant frequencies as shown in Figure 4. To equalize this, we would need to apply a whitening filter.

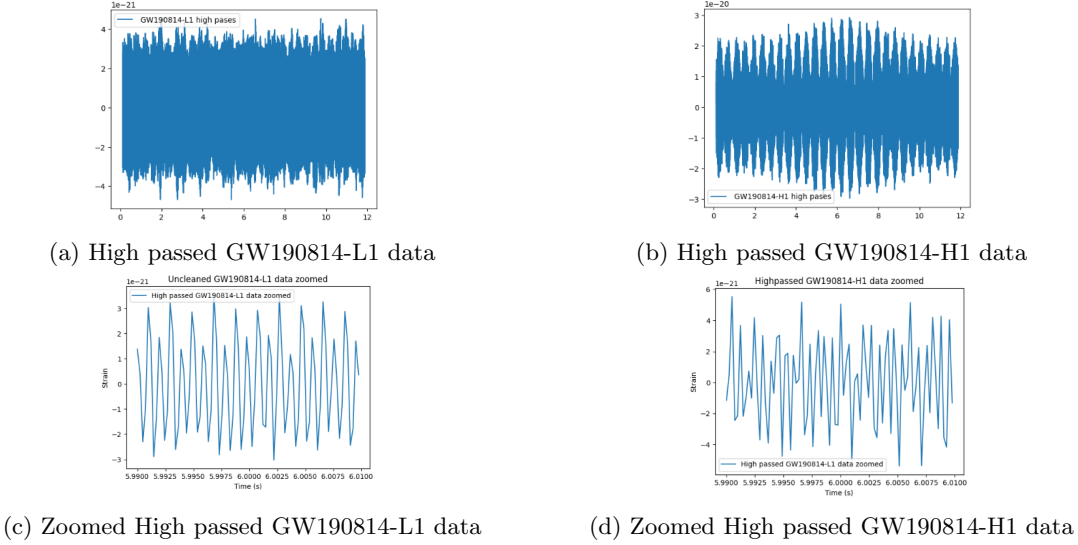


Figure 4: shows high passed GW190814 data

2.6 Power Spectral Density

Before we continue filtering, we will find the power spectral density of the data. In general, PSD provides a detailed view of how the power of a signal is distributed across different frequencies and helps us characterize the behavior of systems. This is crucial for understanding the frequency content of a signal. Figure.6 shows the obtained graphs:

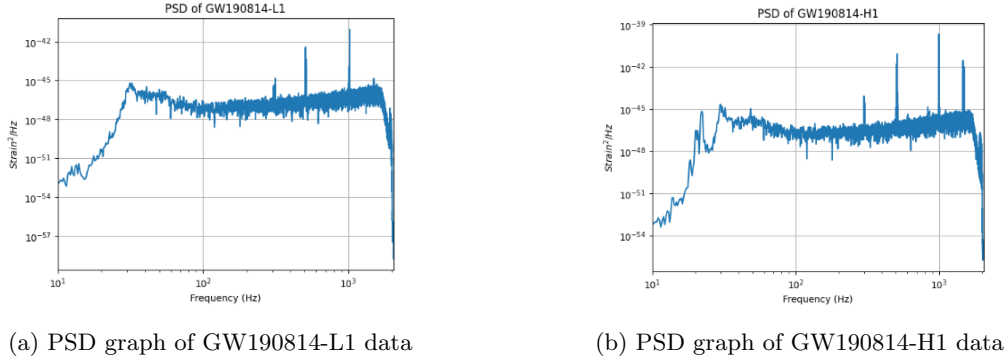


Figure 5: PSD graphs of GW190814 data

2.6.1 What can we see from the PSD graph?

There is a significant amount of noise at low frequencies (orders of magnitude). Note also that there is a large amount of power at a few specific frequencies(which are the exact frequencies previously noticed when doing the Fourier transform). After some research about the source of noises in the LIGO detectors, I found out that the causes for these noises include 60 Hz power line noise, violin modes of the hanging mirrors, and various other instrumental resonances(6). The downturn in power before 2 KHz is due to a low pass filter that was applied before re-sampling the data to 4096 Hz. Therefore, and further filtering is required.

2.7 Whitening the Data

To enhance the detection of deviations from the noise profile, the process of "whitening"(9) the data within a designated frequency range proves valuable. This technique aims to highlight anomalies in the

data by adjusting the power spectral density to achieve a more uniform distribution, ensuring equal contribution from all frequencies.

Figure.6 summarizes our results:

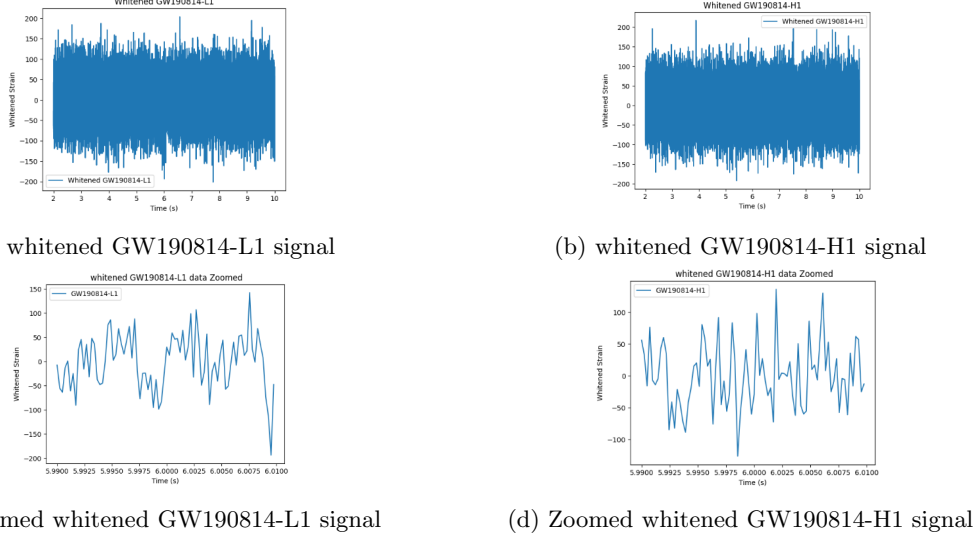


Figure 6: whitened GW190814 signals

As we can see, the shape of the signal started to appear and the noises are now clearly highlighted as anomaly peaks.

2.8 Band pass Filtering

We will now band pass the data around GW150914 between 30 - 250 Hz. This will remove frequency ranges that won't contribute to this kind of signal and make it possible to see the signals in question, as shown in Figure.7

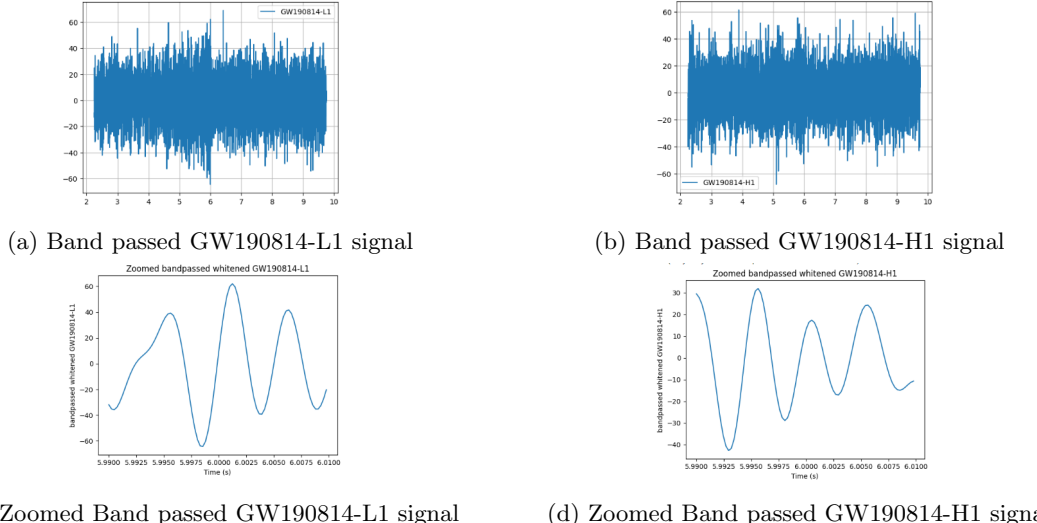


Figure 7: Band passed GW190814 signals

Now, the data is almost cleaned, the wave shape is clearly visible and we can see some coherence in the data. Therefore, the only left step is applying Q-transform and finding the spectrograms.

2.9 Q-transform and Spectrogram

In the realm of mathematics and signal processing, the Constant-Q Transform (CQT) (10) and Variable-Q Transform (VQT), abbreviated as CQT and VQT respectively, offer a transformative approach to analyzing data series in the frequency domain. These techniques, closely tied to the Fourier transform and intricately connected to the complex Morlet wavelet transform(11), find particular relevance in musical representation. Conceptually, the transform operates as a set of filters, denoted as f_k , distributed logarithmically across the frequency spectrum. Each filter, indexed by k , possesses a spectral width δf_k that is a multiple of the width of the preceding filter.

Now, the data is clean and well-visible and our filtering is completed. we can apply Q-transform and then get the spectrogram of our cleaned data and compare it to what we had before. In general, larger Q-values are more appropriate for viewing long-duration features of the data and vice versa. The options here:

- (1) The time spacing for the output image (i.e. 1 ms in this case)
- (2) The number of frequency bins in the output, logarithmically spaced
- (3) The range to maximize over. We'll pick a constant at 8 here Typically higher values will be more appropriate for longer-duration signals
- (4) The frequency range to output

Finally, we plot the spectrogram of the two signals to get the results shown in Figure.8:

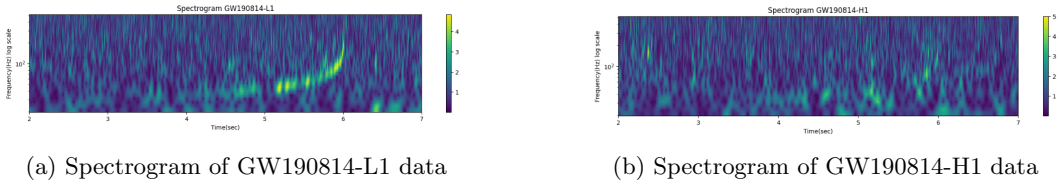


Figure 8: Spectrograms of GW190814 data

2.10 Comparisons

2.10.1 For GW190814-L1:

with our results before cleaning: After cleaning the data, we can finally visualize from the spectrogram a well-visible chirping peak that distinguishes the gravitational waves of merger systems, unlike what we had before cleaning.

with the research paper output: Both our results after cleaning the data and the spectrogram shown in the research paper show very similar results as we can clearly see the wave, its shape, and the chirping peak at the end when the two black holes are merging in both of the spectrograms. Therefore, our analysis and filtering of the 'GW190814-L1' Gravitational waves data was successful and we were able to retrieve the wave and remove most of the disturbing noise resulting from the LIGO detector or external source.

2.10.2 For GW190814-L1:

with our results before cleaning: After cleaning, the spectrogram is now clearer than what we got before it, nonetheless, we couldn't detect the chirping peak even after cleaning the data.

with the research paper output: Both our results after cleaning the data and the spectrogram shown in the research paper show very similar results as we can clearly see the wave and its shape. Even though we couldn't detect the chirping peak in our signal after filtering, the research paper analysis still showed no chirping peak too, which implies that the problem is not in our filtering but rather in the raw data of For GW190814-H1. Therefore, our analysis and filtering of the 'GW190814-H1' Gravitational waves data was also correct.

3 GW170817 Neutron Star Binary System Coalescence

3.1 Characteristics

The GW170817 event(12), detected on August 17, 2017, involved the collision of two neutron stars in the galaxy NGC 4993, situated about 40Mpc away from Earth(130 million light-years). This extraordinary cosmic occurrence, observed through gravitational wave signals by the LIGO and Virgo detectors, showcased the merging of two neutron stars with masses approximately 1.1 and 1.6 times that of the Sun. This collision not only validated the existence of gravitational waves as predicted by Einstein's theory but also marked the first instance where both gravitational waves and electromagnetic radiation (gamma-ray bursts) were simultaneously observed from the same event.

In this segment, our approach will mirror that used for the GW190814 Coalescence. However, our focus now shifts to examining a Binary Neutron Star system, which possesses distinct characteristics from a binary black hole Coalescence. As we delve further into this paper, we aim to elucidate these differences and explore the unique properties associated with this type of celestial event.

3.2 Time domain Visualization

First, we will plot the signal in its time domain, and have a closer look at its data by zooming into small intervals and commenting on what we see. For convenience, we will be dealing with the data from both sources, Livingston(GW170817-L1) and Hanford(GW170817-H1) at the same time.

Figure.9 shows a summary of our results:

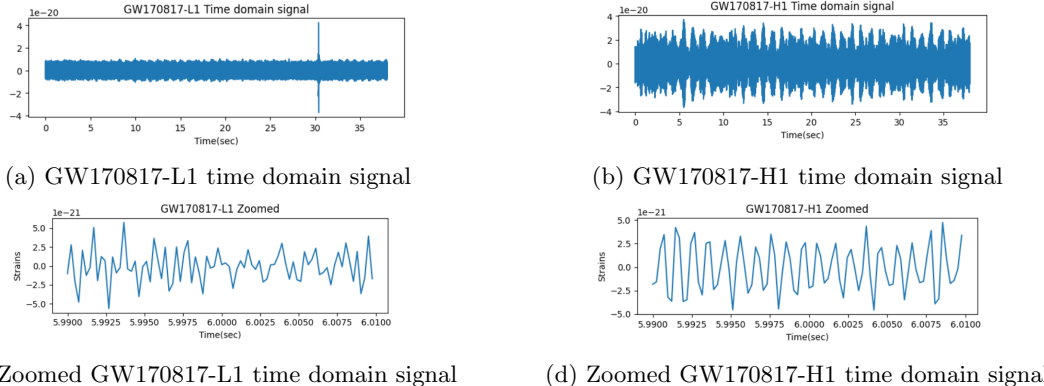


Figure 9: GW170817 time domain signals

3.2.1 Quick Observations

it is significant to notice that even though the Neutron star binary system, GW170817, is located 40 Mpc (almost 130 million light-years) away from Earth which is way closer to us(almost 6 times closer) than the previously studied Black hole system GW190814 (241 Mpc that is almost 7.9 Billion light years away), the gravitational waves data recorded from the two mergers shows a close range of strains magnitude (10^{-21} for both). This makes us conclude that the gravitational waves produced by GW170817 are weaker than those produced by GW190814

A reasonable explanation behind this goes to the fact that Gravitational waves, the result of accelerating masses, are influenced by many factors, one of which is the mass of the body. When comparing a black hole binary system, approximately 10 times more massive than a neutron star system, the larger masses and increased compactness of the black holes significantly impact the emitted gravitational waves. The dynamics of the more massive black hole binary lead to higher velocities and more intense gravitational interactions during a merger, resulting in larger and more energetic gravitational wave signals. This mass difference, combined with the compact nature of black holes, contributes to the expectation of stronger and higher-frequency gravitational waves in such systems. (13)

3.3 Fourier Transform

As we did in GW190814, we will compute the Fourier transforms of the two signals and zoom in to smaller scales, so that we can have an idea of how these two signals behave in the frequency domain. (See Figure.10)

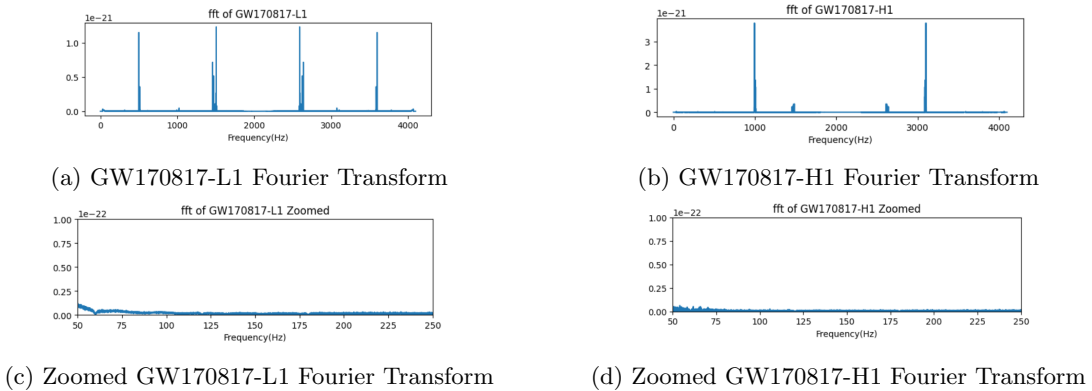


Figure 10: GW170817 Fourier Transforms

3.3.1 Observations

In the analysis of GW190814, the Fourier transforms of signals H1 and L1 reveal distinctive noise patterns, where noise peaks significantly overshadow the signal magnitude. In H1, two dominant noise peaks emerge prominently at frequencies of approximately 1000 Hz and around 3100 Hz, both exhibiting nearly identical magnitudes of approximately $4 * 10^{-21}$. Additional smaller, noise peaks manifest around 1500 Hz and 2500 Hz.

Similarly, the Fourier transform of L1 unveils a more intricate noise profile with multiple peaks, each having magnitudes close to 10^{-21} . Peaks are observed at distinct frequencies, namely 500 Hz, 1500 Hz, 2500 Hz, and 3500 Hz. Notably, smaller peaks with similar magnitudes surface around frequencies of approximately 1500 Hz and 2500 Hz. The prevalence of more spaced peaks in L1, coupled with their comparable magnitudes to that in H1, leads to the conclusion that L1 data exhibits a higher level of noise compared to H1.

Ultimately, we observed a resemblance between the behaviors of both signals, GW170817-L1 and GW170817-H1, and the GW190814 data concerning their most contribution within the frequency range. This contribution was noted to fall within the 50 Hz to 250 Hz range for all signals under examination.

3.4 Windowing and Spectrograms

As we apply to the window, we will be plotting the spectrograms of the two signals. Figure.11 shows the respective Spectrograms:



Figure 11: GW170817 Spectrograms

3.4.1 Observations

While we can spot the chirping peak in both data H1 and L1, Both of the data still show some noise affecting the signal. In H1, we can see that the chirp peak is very dim and is barely visible.

In addition, we can see that there is a dominating frequency peak at $f \approx 480$ Hz in the GW170817-L1 spectrogram that doesn't correspond to the chirping peak nor have anything to do with the gravitational wave expected, therefore it is pure noise detected while recording the data.

Hence, we will follow the same methodology as we did in the GW190814 Coalescence to see if we can have a better visualization and try to get rid of the noise peak in GW170817-L1. From this point onwards, we will apply filters to clean the data and try to extract the signal from the noise.

3.5 Filtering Data from Noise

3.5.1 High pass Filtering

In our processing, we implement a high-pass filter on the data to mitigate low-frequency noise from the instrument. This action notably aligns the dynamic range of the data. Figure 12 shows the application of a high pass filter and a zoom look at the data after high pass filtering:

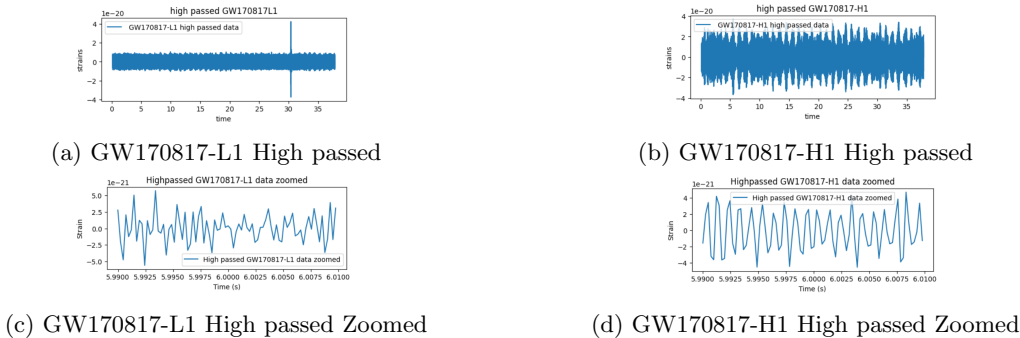


Figure 12: GW170817 High passed data

3.5.2 Whitening the Data

Even after applying high-pass filtering, certain dominant frequencies persist. To address this, a whitening filter application becomes necessary to achieve further equalization and ensure a more balanced distribution of frequencies.

This process involves centering the data, computing the covariance matrix, and performing eigenvalue decomposition. The resulting transformation, applied to the centered data, yields whitened data with a flatter power spectral density. This method is employed to remove biases, balance variances, and ensure a more even distribution of signal strength across frequencies.



Figure 13: GW170817 High whitened data

3.5.3 Band pass filtering

As our last filtering process, we will band pass both data between 30 - 250 Hz. This will remove frequency ranges that won't contribute to this kind of signal and make it possible to see the signal in question. (See Figure.14):

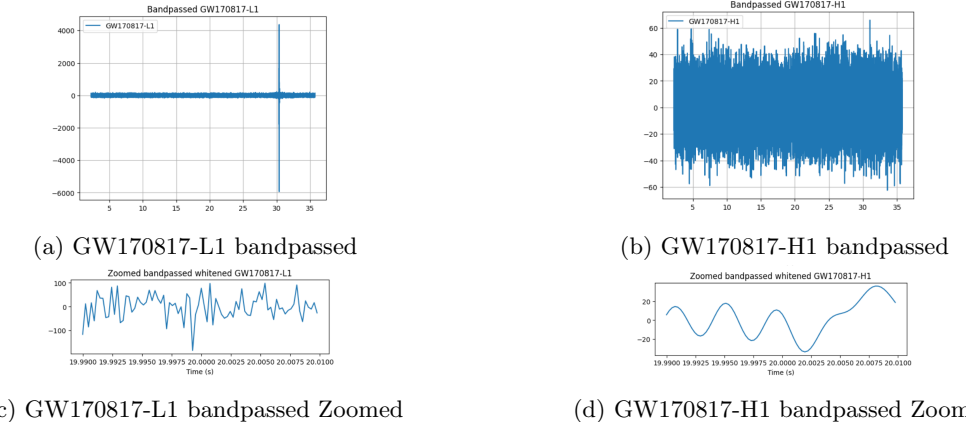


Figure 14: GW170817 bandpassed data

As we can see now, in GW170817-H1 data, there is a coherent signal that matches in phase for a few cycles, while in GW170817-L1, there is still significant noise that hasn't been filtered along the process.

3.5.4 Spectrograms

Finally, we can plot the spectrograms of the signals to see whether our filtering was efficient to better visualize the data (Figure.15):

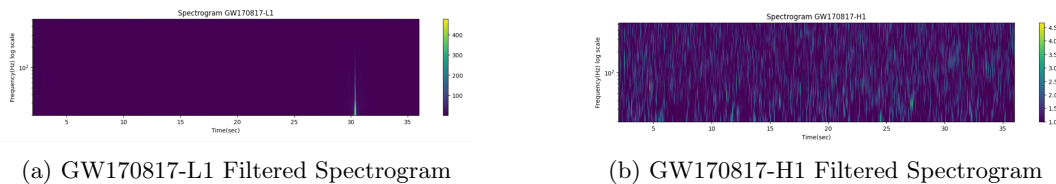


Figure 15: GW170817 Filtered Spectrograms

3.6 Interpretations and comparisons

In the context of the GW170817-H1 spectrogram, although the signal is now clearer, however, we can still see that the chirping peak is hardly visible even after applying some filtering to the data. (Figure 16 shows a hand-drawn highlight on the chirp peak).

In GW170817-L1 we have lost the chirping peak and we can only see a peak of noise located where the chirping peak was supposed to be visible.

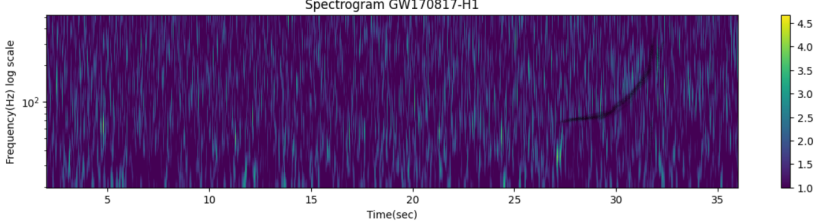


Figure 16: shows the theoretical peak expected drawn by hand in the spectrogram of GW170817-H1 after filtering.

Therefore, the results of our analysis using Q-transform for the GW170817 merger are not as satisfying as it was in the GW190814 merger and are not similar to what we saw in the research paper. This means that Q-transform is not the perfect tool to use for systems like the GW170817

In general, the Q-transform can be a powerful diagnostic. However, note that quieter signals, especially those with **lower masses** will be harder to spot visually(8). While both signals, GW170817 and GW190814 are of similar strain magnitudes, the mass of just one of the celestial bodies in the GW190814 system, in this case, a black hole, is 23.2 solar masses (4), is more than 10 times larger than the masses of the neutron stars found in the GW170817 system(2.7 Solar masses) (12). Therefore, it is expected that we will have better results for the GW190814 Coalescence using Q-transform than that of GW170817.

Another way to study Coalescence is **Matched Filtering**. In general, it is considered a very convenient way to study quieter signals like the ones we have and we will be showing its efficiency as we proceed in this paper

4 Spectrogram Differences between Binary Black Hole Coalescence and Binary Neutron Stars Coalescence

While Both, black hole binary and neutron stars coalescence produce chirping peaks and considerable magnitudes of gravitational waves, the shape of these chirping peaks produced is not the same.

in the context of binary black hole coalescence, the chirping peak seems to be sharper and more rapid in terms of occurrence(approximately from 50 sec to 90 sec in GW190814 as shown in figure.3) while that of neutron star seems to have a longer occurrence duration implying less sharpness in the peak(approximately from 200 sec to 480 sec as shown in figure.11). This could probably be explained by understanding the natural differences between these two celestial bodies.

In black hole coalescence, the higher masses and intense gravitational forces create sharper, more rapid chirping peaks during the brief in-spiral phase, due to the swift orbital decay of these massive objects. Interestingly, neutron star mergers involve less massive yet highly dense entities (13), resulting in a slower evolution of gravitational wave frequency changes. Consequently, the chirping peaks in neutron star coalescence tend to appear more gradual and less sharp than those observed in black hole mergers

5 Matched Filtering Method

5.1 Definition

Matched filtering(14) is a powerful signal extraction technique used when the signal of interest is buried in noise or weak. It relies on correlating a known simulated waveform, representing the expected signal, with the data obtained from the detector. The correlation process produces a signal-to-noise ratio(SNR) time series, where the presence of a signal is realized by when peaks above a threshold are spotted. Maximizing the SNR and aligning it with the original signal help us extract the signal in interest from noise. Since we are dealing with signals that are both quiet and noisy, matched filtering might be one of the solutions to extract the gravitational waves of the Binary systems of interests

In this section, we will explore the efficiency of using match filtering on four different Binary black hole systems: GW150914-H1, GW151226-H1, GW170814-L1, and GW170823-H1.

The process(8) will consist of the following steps:

- 1) Testing the effect of the binary system component masses and distance from Earth on the simulated signal
- 2) Filtering and conditioning the raw data of the merger.
- 3) Creating a simulated signal
- 4) Finding the Power Spectral Density(PSD) and the Signal-to-Noise-Ratio(SNR) of our simulated signal
- 5) Aligning and Subtracting the simulated signal from the original data
- 6) Plotting the spectrograms

5.2 Binary Systems Characteristics:

5.2.1 Binary Black hole systems Characteristics

We will start by first giving brief characteristics of the merger black holes we will be studying:

Note:

Mpc = Megaparsecs

1 solar mass(M_{\odot}) = mass of our sun

1 Mpc = 3261563.7769443 Light years

GW150914-H1 (15):

Nature: Black hole binary system.

Mass1: $36(+5,-4) M_{\odot}$

Mass2: $29(+4,-4) M_{\odot}$

Distance from Earth: $410(+160,-180)$ Mpc

GW151226-H1 (16):

Nature: Black hole binary system.

Mass1: $14.2(+8.3,-3.7) M_{\odot}$

Mass2: $7.5(+2.3,-2.3) M_{\odot}$

Distance from Earth: $440(+180,-180)$ Mpc

GW170814-L1 (17):

Nature: Black hole binary system.

Mass1: $30.5(+5.7,-3.0) M_{\odot}$
 Mass2: $25.3(+2.8,-4.2) M_{\odot}$
 Distance from Earth: $540(+130,-210) \text{ Mpc}$

GW170823-H1 (18):

Nature: Black hole binary system.
 Mass1: $39.5(+11.2,-6.7) M_{\odot}$
 Mass2: $29.3(+6.7,-7.8) M_{\odot}$
 Distance from Earth: $1940(+970,-900) \text{ Mpc}$

5.3 Model used

To generate a simulated signal, we are using the **waveform approximate method**. i.e: **SEOBNRv4-opt** (19) model. After some manipulations and filtering, This signal is supposed to later mimic the chirping peak of our merger system and help us extract the chirping peak signal successfully from the raw data Detected by LIGO. **Further illustration on the model and its parameters can be found in GW150914-H1 Jupyter notebook**

The **SEOBNRv4-opt** model is firmly grounded in Einstein's theory of general relativity, providing a mathematical framework to describe the gravitational wave emissions from binary black hole mergers based on the principles established by Einstein. General relativity predicts the existence of gravitational waves as ripples in space-time caused by accelerating masses. The model incorporates the Effective-One-Body (EOB) formalism, which is a theoretical approach to solving Einstein's field equations for binary systems by combining analytical insights with numerical relativity simulations. The post-Newtonian expansions used in the model are derived from general relativity, representing a perturbative series that approximates the dynamics of the binary system. Since the mathematical theories behind the model are out of this paper's scope, we won't be diving deeply into the detailed equations behind it, but we need to note that to benefit from the model we have to take into account the model's key parameters behind the simulation: Masses of the binary (in solar masses), the time between samples (in seconds), the starting gravitational-wave frequency (Hz) and name of the approximate we'd like to generate, in this case, 'SEOBNRv4-opt'. Further explanation about it can be found in the attached Jupiter notebooks.

5.4 Effect of Mass and Distance on Simulated Signal

In this section, we will be testing how the simulated signals by our model vary as the masses of the binary system and distance from Earth change. To do that we will fix all the parameters except that of interest and plot the corresponding graphs(**Check GW150914-H1 Jupyter notebook for the code**). Figure. 17 shows the obtained results:

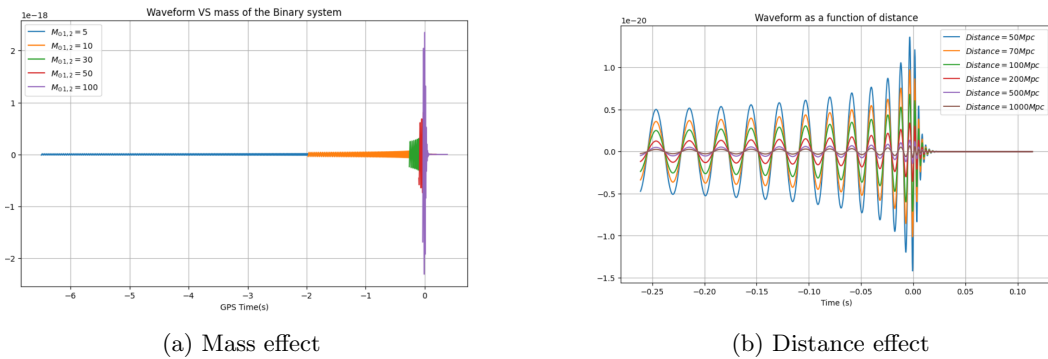


Figure 17: Mass and distance effects on simulating signals

As depicted in Figure 17, the waveform length exhibits an increase in lower-mass binary mergers. This trend aligns with the observed behaviors in the GW190814 black hole system and the GW170817 neutron star binary system. In the latter case, the gravitational wave from the neutron star binary

system, characterized by lower masses, had a more prolonged duration compared to that from the black hole binary system, which had masses almost ten times larger.

Furthermore, the magnitude of detected waveform strains decreases as the distance from the source increases and vice versa. This aligns with findings from our analyses of the GW190814 and GW170817 systems, demonstrating a similar pattern—more massive binary systems at greater distances exhibit wave magnitude detections comparable to smaller in-mass binary systems closer to Earth.

Therefore, the hypothesis presented in Section 4 regarding the differences in chirping peak sharpness between GW190814 and GW170817 stands validated.

5.5 Raw data Filtering

As we did with the previous two systems GW190814 and GW170817 data, we first apply high pass filtering to get rid of the low-frequency noise. After that, we will remove the first and last 2 seconds of the high-passed data to avoid the spikes created at the boundaries due to high-pass filtering. Figure.18 summarizes the signals obtained for the four mergers.

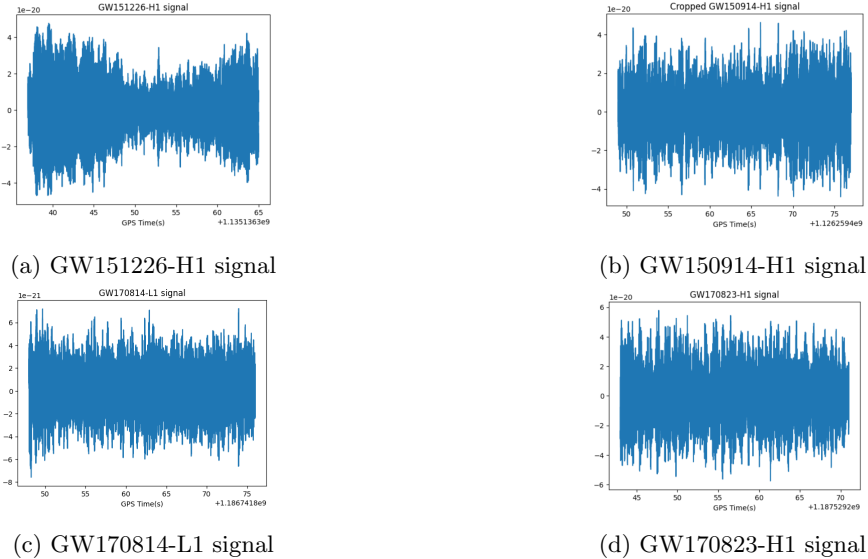


Figure 18: Mergers original signals

5.6 PSD graph

Optimal matched filtering requires weighting the frequency components of the potential signal and data by the noise amplitude. We can view this as filtering the data with the time series equivalent of $1 / \text{PSD}$. To ensure that we can control how much this filters the data, we window the time domain equivalent of the PSD to a specific length. Figure.19 shows the PSD graphs of our mergers. (next page)

5.7 Simulating Mergers' Signals

In general, matched filtering involves laying the potential signal over your data and integrating (after weighting frequencies correctly). If there is a signal in the data that aligns with your 'simulated', you will get a large value when integrated over. Since we already know our merger system, we then have the key parameters discussed above, and we'll use them now to build the model to simulate similar conditions to our system(see Figure 20). We assumed equal masses of the two bodies in each system as they overlap in uncertainties

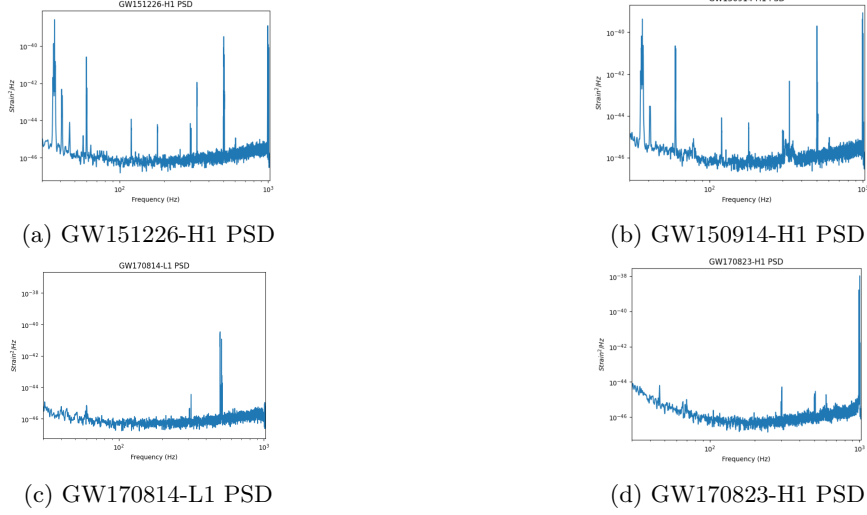


Figure 19: Mergers' PSD graphs

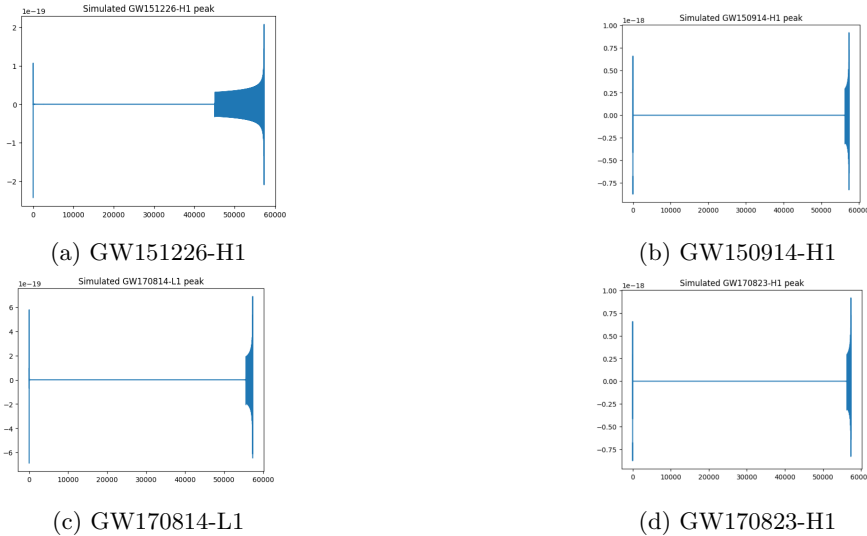


Figure 20: Mergers' simulated signals

5.8 SNR of Simulated Signals

Now that we have both our simulated signals and the PSD of our original data, we can now find the signal-to-noise for our simulated signals. Further illustrations can be found in the attached Jupyter notebooks, and the summarized results are shown in Figure 21.

5.9 Alignment and Subtraction

In principle, Unique standing peaks in the SNR graphs indicate the presence of the signal of interest, and to exploit this opportunity we have to align and then subtract our simulation from the original data. After that, both, the simulated signal and the original data will go through whitening and then band pass filtering to finally obtain the results in Figure 22. (next page)

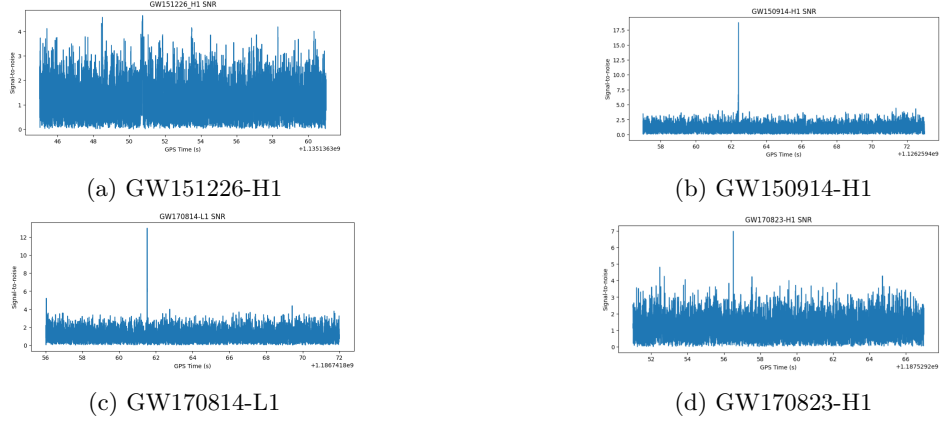


Figure 21: Mergers' simulated signals SNR

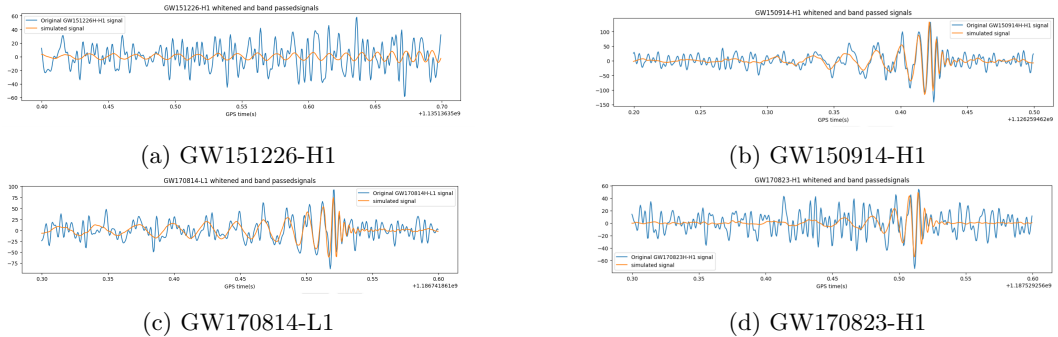


Figure 22: Mergers' simulated and original whitened signals

5.10 spectrograms

Finally, we now have both, the original signals and the simulated signals that are aligned and coherent with the original ones for the four mergers, and all that is left is to test how accurate our signals are by displaying the spectrogram of the subtraction of the simulated signals from the original one and see if we can remove the chirping peaks in all mergers. Figures 23, 24, 25 and 26 show the obtained results.

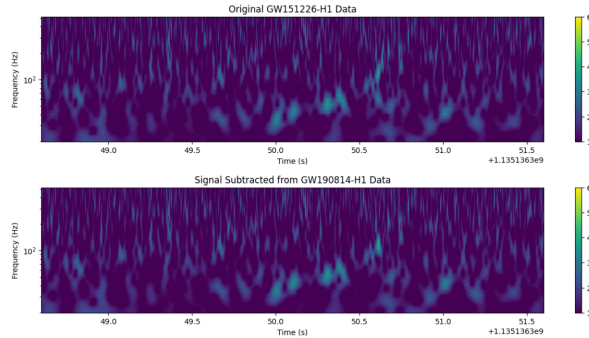


Figure 23: GW151226-H1 spectrograms

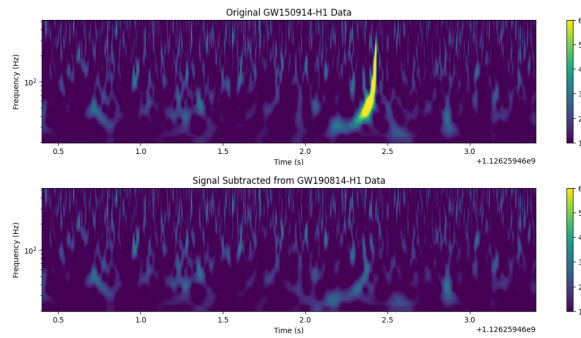


Figure 24: GW150914-H1 spectrograms

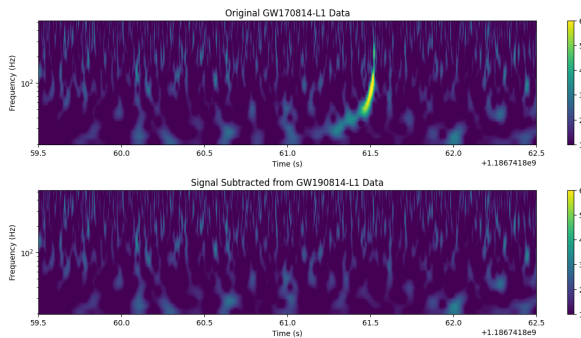


Figure 25: GW170814-L1 spectrograms

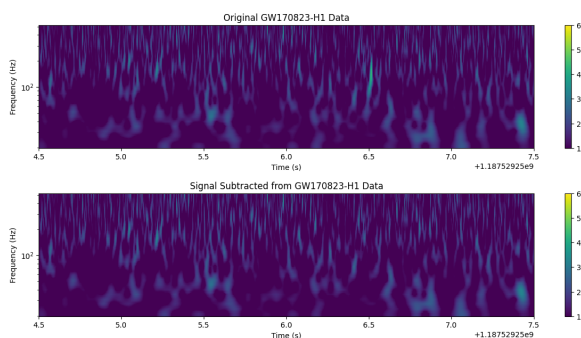


Figure 26: GW170823-H1 spectrograms

5.11 Interpretations

In the analysis of GW170814-L1 and GW150914-H1(Figures.24 and 25), a notable observation is the complete disappearance of well-defined chirping peaks in the original data histogram after subtracting the simulated signals generated by our models. This suggests that the simulated signals align remarkably well with the actual gravitational wave signals from clean mergers. Even in cases where a very faint chirping peak was present, as in GW170823-H1(See Figure.26), our model accurately extracted this signal, and the faint peak can no longer be seen after subtraction. Furthermore, examining the GW151226-H1 spectrogram(Figure 23) revealed no detectable chirping peak before or after subtraction. Since the primary purpose of Matched Filtering is to simulate the pure signal rather than the accompanying noise, the lack of improvement in the data post-subtraction was because the original signal of the merger is not captured by the raw original data file and therefore, matched filtering won't improve the results. This robust demonstration underscores the efficiency of Matched Filtering in extracting both strong and weak signals from the noise in gravitational wave data, emphasizing its critical role in enhancing sensitivity in gravitational wave analysis.

6 Conclusion

In conclusion, our in-depth analysis of GW190814 and GW170817 data from LIGO detectors has shown distinct features of gravitational wave signals originating from binary black holes and neutron star mergers. The observed challenges in extracting neutron star signals using Q-transform techniques emphasize the need for different signal processing approaches than Q-transform for such systems.

In contrast, the application of matched filtering has proven to be a robust technique for extracting buried and quiet signals, even in scenarios where noise overwhelms the original signal.

Furthermore, the comparative analysis underscores the importance of understanding the unique characteristics of different astrophysical systems. The success of matched filtering in extracting signals from both quiet and noisy events suggests its versatility and efficacy in mitigating challenges associated with diverse gravitational wave sources.

7 References

- 1) Sources and types of gravitational waves. (n.d.). Retrieved from <https://www.ligo.caltech.edu/page/gw-sources>
- 2) (N.d.). Retrieved from <https://flexbooks.ck12.org/cbook/ck-12-middle-school-earth-science-flexbook-2.0/section/1.1/>
- 3) Richardson, L. (2019). The sliding window discrete Fourier transform. Retrieved from: <https://kilthub.cmu.edu/articles/thesis/The-Sliding-Window-Discrete-Fourier-Transform/8191937>
- 4) R. Abbott, et al. “GW190814: Gravitational Waves from the Coalescence of a 23 Solar Mass Black Hole with a 2.6 Solar Mass Compact Object.” *The Astrophysical Journal Letters*, iopscience.iop.org/article/10.3847/2041-8213/ab960f.
- 5) Lecture 7 -the Discrete Fourier Transform - University of Oxford, www.robots.ox.ac.uk/~sjrob/Teaching/SP/l7.pdf. Accessed 22 Dec. 2023.
- 6) Gwastro. “Gwastro/Pycbc-Tutorials:(Tutorial-1) Learn How to Use PYCBC to Analyze Gravitational-Wave Data and Do Parameter Inference.” GitHub, github.com/gwastro/PyCBC-Tutorials. Accessed 22 Dec. 2023.
- 7) “Understanding and Implementing the Sliding DFT - Eric Jacobsen.” DSP, www.dsprelated.com/showarticle/776.php. Accessed 22 Dec. 2023.

- 8) Gwastro. "Gwastro/Pycbc-Tutorials: Learn How to Use PYCBC to Analyze Gravitational-Wave Data and Do Parameter Inference." GitHub, github.com/gwastro/PyCBC-Tutorials. Accessed 22 Dec. 2023.
- 9) bronze badges, et al. "What Is Spectral Whitening?" Signal Processing Stack Exchange, 1 Sept. 1959, dsp.stackexchange.com/questions/10183/what-is-spectral-whitening
- 10) "Constant-Q Transform." Wikipedia, Wikimedia Foundation, 22 July 2023, en.wikipedia.org/wiki/Constant-Q-transform.
- 11) "Morlet Wavelet." Wikipedia, Wikimedia Foundation, 20 Dec. 2023, en.wikipedia.org/wiki/Morlet-wavelet.
- 12) Collaboration, The LIGO Scientific, and The Virgo Collaboration. "GW170817: Observation of Gravitational Waves from a Binary Neutron Star Inspiral." arXiv.Org, 16 Oct. 2017, arxiv.org/abs/1710.05832.
- 13) By. "Neutron Star vs Black Hole (Similarities and Differences)." Scope The Galaxy, scopethegalaxy.com/neutron-star-vs-black-hole/. Accessed 22 Dec. 2023.
- 14) Introduction to Matched Filters - Crewes, www.crewes.org/Documents/ResearchReports/2002/2002-46.pdf. Accessed 22 Dec. 2023.
- 15) "First Observation of Gravitational Waves." Wikipedia, Wikimedia Foundation, 19 Nov. 2023, en.wikipedia.org/wiki/First-observation-of-gravitational-waves.
- 16) "GW151226." Wikipedia, Wikimedia Foundation, 13 May 2023, en.wikipedia.org/wiki/GW151226.
- 17) "GW170814." Wikipedia, Wikimedia Foundation, 22 Mar. 2022, en.wikipedia.org/wiki/GW170814.
- 18) "GW170823." GW170823 Detail Page, gwosc.org/eventapi/html/GWTC-1-confident/GW170823/v1/. Accessed 22 Dec. 2023.
- 19) ArXiv:1611.03703v3 [GR-QC] 29 Mar 2017, arxiv.org/pdf/1611.03703.pdf. Accessed 22 Dec. 2023.